AIAA JOURNAL
Vol. 40, No. 7, July 2002

Mixing of Transversely Injected Jets into a Crossflow Under Low-Density Conditions

T. M. Muruganandam,* Srihari Lakshmi,† A. A. Ramesh,† S. R. Viswamurthy,† R. I. Sujith,‡ and B. M. Sivaram§
Indian Institute of Technology Madras, Chennai 600 036, India

The objective of this study is to investigate experimentally the mixing of transversely injected jets into a crossflow under low-density conditions. This study has application in nitrogen-diluted subsonic chemical oxygen iodine lasers. The investigation was performed nonintrusively, using planar-laser-induced fluorescence. A frequency doubled Nd:YAG laser was used as the excitation source, and the iodine fluorescence was imaged using a charge-coupled device camera. Experiments were performed for a variety of crossflow velocities and injection pressures. A parameter, degree of unmixedness, which was defined using variance of the image intensities, was used to quantify the mixing. Mixing distance was defined as the location downstream of which the degree of unmixedness did not exceed 0.05. The mixing distances obtained were correlated using the ratio between the momentum flow rates of the injected jets and the crossflow. The mixing distances were linearly dependent on this ratio until a value more than which the jets mixed almost at the injection location. This linearity depended on the injection configuration. The correlation was found to be a weak function of the injector hole diameter. Diffusion is the main mixing mechanism in this low-Reynolds-number flow regime, and thus the spatial distribution of the injector holes in the array played an important role in mixing.

Introduction

JETS in confined crossflow have been the subject of considerable scientific and practical interest. Such flows occur in a number of areas important in fluid mechanics and combustion. For example, in a gas turbine combustor the mixing of fuel and air is of critical importance to the combustor performance and reduction of emissions. Another example is in the dilution zone of a conventional combustor and the mixing zone of a stages combustor such as the rich-burn/quick-mix/lean-burn combustors. Research on jets in crossflow has been summarized well in the review papers by Margason[1] and Holdeman.[2] Results from rectangular and annular configurations have been reported recently by a number of researchers.[3–10]

All of the investigations were performed at atmospheric pressure or at higher pressures. Despite the extensive treatment in the literature, not much work has been done in the investigation of jets in crossflow under conditions of low pressure. Such an application occurs in chemical oxygen iodine lasers (COIL), in which the mixing of transversely injected streams of iodine carried by a carrier gas where a crossflow of singlet oxygen occurs.

Gas lasers such as COIL still dominate when very high powers, high beam quality, and high coherence properties are required, despite the many attractive features, in particular, the possibility of an all-solid system design, shown by solid state and diode lasers. The main candidates are the HF, the CO_2, the CO, and the oxygen iodine laser. The chemical oxygen iodine laser[11–13] is of immense interest, as a very powerful laser, capable of producing megawatts of continuous power, at a short wavelength (1315 nm). The main merits of COIL are its simple and readily available starting reactants and nontoxic end products and the absence of high-voltage power supplies.

There are two distinct types of chemically pumped oxygen iodine lasers: subsonic and supersonic. In subsonic lasers the main flow velocities are limited to about 10–20 m/s, whereas in the case of supersonic lasers the flow velocities are of the order of 400–500 m/s for nitrogen-diluted systems and up to 1000 m/s for helium-diluted systems.

COIL produces electronically excited atomic iodine, the source of radiative and stimulated emission, through a series of chemical reactions. The source of energy in this laser is the chemical reaction between the basic solution of hydrogen peroxide and chlorine gas, which produces electronically excited singlet oxygen [$O_2(^1\Delta)$]. Molecular iodine is injected into the gas flow, and through a series of electronic-vibrational collisional energy transfers, I_2 is dissociated, producing ground state iodine [$I(^2P_{3/2})$]. A resonant collisional energy transfer from $O_2(^1\Delta)$ to $I(^2P_{3/2})$ produces the electronically excited $I(^2P_{1/2})$, commonly denoted as I^*. This I^* emits a photon at a wavelength of 1315 nm to provide lasing in the COIL.

Avizonis and Truesdell,[11] in their excellent review paper, described the evolution of COIL. They have highlighted the unique characteristics of COIL that have allowed it to develop into a high efficiency and robust system.

The process of iodine dissociation, popular inversion, and lasing in the chemical oxygen iodine lasers are affected by the mixing between the flows of oxygen and injected iodine. Barmashenko et al.[14] studied the effect of mixing on the operation of COIL by theoretically applying simple, one-dimensional leaky stream tube model and compared the results to available experimental data. They reported good qualitative agreement with the experimental results for both subsonic and supersonic COIL. Barmashenko and Rosenwaks[15] investigated the power dependence of the supersonic chemical oxygen iodine laser on iodine dissociation. Numerical modeling shows that maximum power is achieved at low values of iodine flow rate, when iodine is not completely dissociated before the resonator. The performance of high-pressure COIL was modeled using computational fluid dynamics (CFD).[16–18]

Planar-laser-induced fluorescence (PLIF) is an attractive technique for concentration measurements in liquid and gaseous flows as it is nonintrusive and effectively instantaneous and provides concentration information in a whole plane without integration along the line of sight. Its use of molecular markers avoids problems of particle lag in fluid flow and allows high spatial resolution measurements with minimal alteration of the flow conditions. The flow is illuminated using a laser sheet, and images are formed from light emitted by the molecules in the flow.[19]

Presented as Paper 2000-0203 at the AIAA 38th Aerospace Sciences Meeting, Reno, NV, 10–14 January 2000; received 18 February 2000; revision received 19 November 2001; accepted for publication 21 December 2001.

*Graduate Student, Department of Aerospace Engineering; currently Graduate Research Assistant, Georgia Institute of Technology, Atlanta, GA 30332. Member AIAA.
†Undergraduate Student, Department of Aerospace Engineering.
‡Assistant Professor, Department of Aerospace Engineering. Member AIAA.
§Professor, Department of Physics; deceased 25 December 1999.

Laser-induced fluorescence (LIF) of iodine seed molecules can be used for both flow visualization and accurate measurements of gas dynamic properties. Hiller and Hanson[20] give a review of the use of iodine as a tracer gas in experimental fluid mechanics. Iodine is a popularly used seed molecule for LIF measurements in noncombusting gas flows.[21,22] It conveniently absorbs in the visible region of the spectrum (for example, green 514.5-nm line of the argon ion laser or 532 nm of the frequency doubled Nd:YAG laser); fluoresces in visible yellow; has reasonable values for vapor pressure, absorption cross section, and fluorescence yield; and is only mildly toxic.

Bohn[23] has presented a review of the German work related to COIL technology. A description of the laser test facility and the latest performance data is presented and compared with the international state of the art. The paper reports that LIF measurements have been performed. However, no data are presented.

In the context of COIL, injection, and mixing of iodine, Schall[24] investigated the injection of iodine vapor into a duct flow experimentally and numerically. LIF was used to visualize the progress of spreading of the iodine and its distribution homogeneity along the duct. The paper concluded that perpendicular injection from the walls is undoubtedly the most efficient means of injection for obtaining the shortest mixing lengths. However, the paper gives scant data.

In this context this paper describes an experimental investigation of the mixing of transversely injected choked jets into a crossflow under low-density conditions. The investigation is performed nonintrusively, using PLIF. The effects of injector hole configurations, hole diameters, crossflow velocities, and injection pressures on mixing have been quantified in this paper. The investigation of nonchoked injection is being performed currently and will soon be presented elsewhere.

Experimental Setup

The experimental setup was designed to simulate the flowfield in a subsonic COIL. The schematic of the various parts of the experimental setup is shown in Fig. 1. In this study the fluid phenomenon alone was investigated and not the lasing action. Therefore, dry air whose properties, such as specific heat ratio, gas constant, molecular weight, etc., are comparable to that of singlet oxygen was used for the crossflow instead of singlet oxygen.

The main flow of air is from a dry air cylinder. The iodine vapor was generated in an iodine cell and was carried by nitrogen into an injection manifold. The test section was a rectangular chamber made of four glass walls with the top and bottom walls made of mild steel flanges. Inside this chamber there were two parallel surface ground plates made of mild steel. These plates were coated with nickel to minimize the corrosion caused by iodine. The plates were 650 mm long and 49.5 mm wide. The spacing between the plates was 10 mm. The plates along with the side glass walls formed a rectangular duct

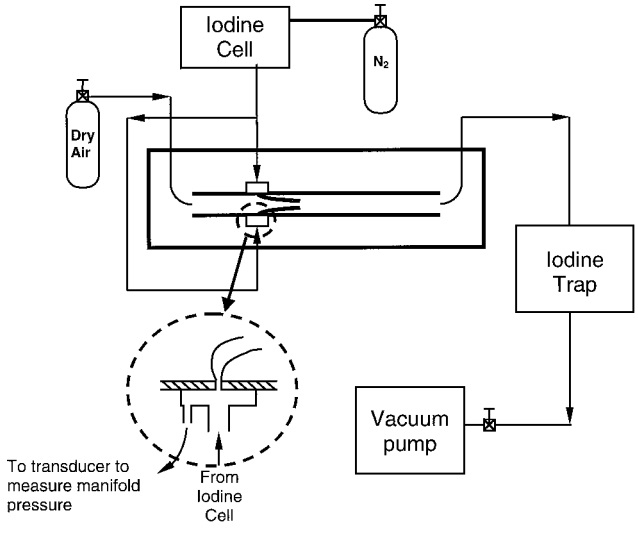

Fig. 1 Schematic of the experimental setup.

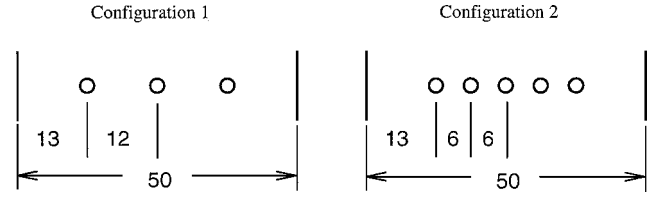

Fig. 2 Different hole configurations used in this study (all dimensions in millimeters). For both these configurations two hole sizes (0.7- and 1-mm diam) were used.

of cross section 10 × 50 mm. The middle portion of this rectangular duct was the test section for this study.

The injection holes were placed in a row at 200 mm from the beginning on each of the plates, where the flow is fully developed for all of the flow conditions considered.[25] Two different hole diameters, 0.7 and 1 mm, and two different injector hole configurations, 12 mm (3 holes across the width) and 6 mm (5 holes across the width), as shown in Fig. 2, were used in this study (two injector hole diameters for each injector configuration). The injection holes are simple straight holes through the thickness. Efforts were made to align the injector holes perfectly. However, because of limitations in the machining capabilities some of the holes in the injector array were not perpendicular to the plate, resulting in a deviation of 2–3 deg from the normal.

These holes are supplied through a manifold into which the iodine vapor along with the carrier gas (nitrogen) was supplied from the iodine cell. These manifolds were rectangular chambers of stainless-steel, 10 mm wide (see inset in Fig. 1). Nitrogen carrying the iodine vapor was supplied through a stainless-steel tube to each of these manifolds. There was a pressure tapping on the manifold to measure the injection pressure, which is the stagnation pressure for the jet.

The pressure in the test chamber was monitored by a Pirani gauge. The pressure in the injection manifold was measured using a silicon piezoresistive pressure transducer. The volume flow rate of air entering the test section was monitored using a thermal flow meter. Test section pressures required for this study were of the order of a few torrs. The flow rates are in the range 0.148–0.444 mmol/s (200–600 standard cm^3/min volume flow rate, which corresponds to 2–6 m/s at 1 torr in the test section of 10 × 50 mm), and the flow was generated by a vacuum pump of 4000-lpm capacity.

The flowfield was illuminated by a frequency doubled Nd:YAG laser. The line width of the laser was around 1–2 cm^{-1}, and thus it excited several lines in the R and P branches of the B → X transition of the iodine molecule[26]: R(56)(36-0) line at 18,788.348 cm^{-1}, the P(83)(33-0) and R(134)(36-0) lines at around 18,787.814 cm^{-1}, and the P(53)(32-0), P(103)(34-0), and P(159)(39-0) lines at around 18,788.453 cm^{-1}. Nitrogen molecules in the system will broaden the iodine absorption spectrum significantly. Because the excitation employed here is relatively broadband, this will not have a significant bearing on the results.

The short Q-switched pulse width (17 ns) ensures that the timescale involved in probing the flow was much less than the flow timescales. Thus, the flow was frozen in the image at each cross section. The beam from the laser source was expanded to a diameter of approximately 12 mm using a pair of spherical lenses. A cylindrical lens of focal length 1 m was then used to focus the beam to a line. The long focal length enables the beam waist to remain uniform through out the test section (for a length of 50 mm). The sheet thickness was found to be around 500–600 μ.

The fluorescence pictures were acquired using a charge-coupled device camera, which was positioned next to the test chamber at an angle of 35 deg to the flow direction. Thus, the images were slightly elongated in the horizontal direction. However, this did not affect the calculations as the full flowfield was mapped at the same cross section. Each pixel in the image represents an area of 0.21 × 0.16 mm of the flowfield. Refer to Fig. 3 for a schematic of the full optical setup. The aperture was kept fully open for allowing maximum fluorescence signal into the camera. It was also ensured that none of the camera pixels were saturated.

Because the aperture was fully open, the depth of focus was small. The depth of focus was found to be around 23 mm (for the setup

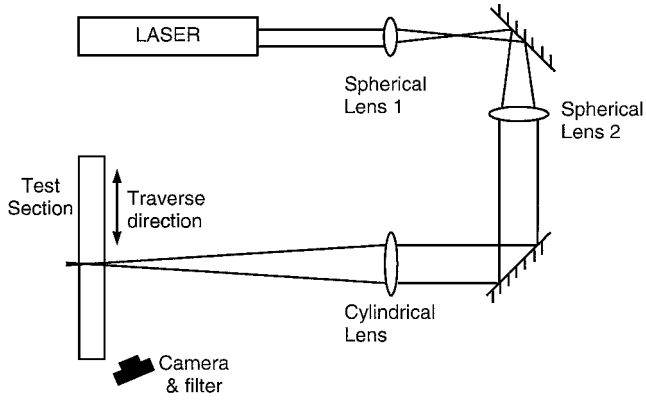

Fig. 3 Schematic of the optical setup for imaging PLIF cross sections.

used). Thus the focal plane covered around 42 mm, that is, only a part of the width of the test section. This implies that near the glass walls in any cross-section image the flow plane to be visualized was slightly out of focus. Though the focal plane was around 23 mm thick, the volume probed was much smaller because the laser sheet illuminating the flowfield was very thin.

Iodine molecules emit a fluorescence spectrum that is predominantly yellow when excited by green light of wavelength 532 nm (several lines between 550 and 590 nm but broadened by nitrogen carrier to give a broadband fluorescence spectrum). A long-pass filter was used to filter all of the wavelengths less than 560 nm (cutoff wavelength) including the scattered green light from the incident radiation. A traverse mechanism was used to translate the test section along the streamwise direction with respect to the optical setup.

Image Processing

There was a high-frequency noise superimposed over the whole image. This was eliminated by passing the image through a low-pass spatial filter. A standard 7×7 matrix averaging of the pixels with weights given to each pixel in the matrix was adopted.[27] This eliminated the high-frequency noise without altering the features of the flow, which were of a much lower spatial frequency. The Reynolds number of the crossflow was of the order of 4–12, and that of the jets ranged from 92 to 265. Thus the flow was strictly laminar, and diffusion played an important role in this low-pressure flow. This ensured that the transported quantities are not distributed with very high gradients or sharp changes. Thus, the use of low-pass spatial filter to alter the image did not affect the flow quantification.

There was an observable spatial variation of the laser sheet intensity in the experiment, and this can cause an error in the quantification. This variation could be because the beam intensity profile for the Nd:YAG laser is not top-hat. It could also be caused by nonuniformities in the laser crystals or lenses used or possible dust on mirror surfaces, etc. This variation in illumination intensity was corrected by dividing each of the flow images by the flat-field image. It can be noticed that the average intensity value of the image changes because of this correction by a factor of ratio of average of flat-field image to that of the original image.

Because the experiments spanned over a definite time period and there was some time difference in acquiring images at different locations, there could have been a variation in the laser intensity over the time period. This could have been caused by variation in the voltage input, the ambient temperature, or the temperature of the crystals involved. Also, as described in the preceding paragraph, there was a scaling factor added to the images by correcting with the average of the flat image. In addition, the iodine concentration in the injected gases could change as a function of time. The sum of the intensities of all of the pixels is proportional to the number density of the injectant species and hence should be conserved from location to location. Therefore a correction was introduced by multiplying each of the images by a suitable factor to make the sum of the intensity values (and therefore the average intensities) uniform for a certain flow condition.

Data Reduction

The fluorescence intensities are proportional to the number density of the fluorescent species. Acquiring the fluorescence intensities in a plane, the relative distribution of the iodine number density can be determined. Because the average image intensity for a particular flow condition was kept constant, any variation in the total amount of iodine or the illumination in the flowfield was eliminated. Thus the number density contours given by the images can be translated to the relative injectant mole fraction distribution in the flowfield.

The images thus obtained and processed can be used for quantifying mixing. Mixing is quantified through a parameter called the degree of unmixedness, defined by Liscinsky et al.[9] and Holdeman et al.[10] This is given by degree of unmixedness

$$U = \frac{\sum_{\substack{x=1 \\ y=1}}^{\substack{x=x_{\max} \\ y=y_{\max}}} [I(x, y) - I_{\text{ave}}]^2}{N I_{\text{ave}} (I_{\max} - I_{\text{ave}})}$$

where $I(x, y)$ denotes the intensity value of a pixel (x, y). I_{ave} is the average of the intensity values of all of the pixels in the image. $I_{\max}$ is the maximum of the intensities of pixels among all the cross-section images for a given flow condition. N here is the number of pixels in each image. Intensities of the pixels in the image will be equal to the average of the image when complete mixing is achieved. Because variance is a measure of deviation from the mean value of the distribution, it is used for studying the extent of the nonuniformity or the degree of unmixedness. Because the images are corrected such that they have the same average, the variations in iodine seeding in the flow or the temporal variations in the laser intensities are accounted for. This is justified by the fact that we operate in the linear regime of iodine fluorescence.

Results and Discussion

The flow rates for the crossflow were 0.148, 0.222, 0.296, 0.370, and 0.444 mmol/s (200, 300, 400, 500, and 600 standard cm^3/min). The uncertainty in the measurement was 0.74 μmol/s (1 standard cm^3/min). These flow rates translated to velocities of 2.3, 3.2, 3.9, 4.6, and 5.6 m/s, respectively, in the test section for a test section pressure of 1 torr. The chamber pressure was around 1–3 torr for various flow conditions. The experiments were performed for injection stagnation pressures of 7, 12, and 14 torr. The uncertainties in the chamber and injection pressure measurement were 0.1 and 0.76 torr, respectively.

The injection holes were choked for these pressure conditions. Thus the injection velocities were constant (264 m/s corresponding to Mach 1 for a stagnation temperature of 308 K). However, the mass flow rates and densities were dependent on the injection pressure and the injector configuration.

The mole fraction maps were obtained for all of the injector configurations for the flow conditions just described. Though the images are stored as 16-bit gray scale images, they are presented here in 8-bit gray scales, with the "gray code" next to the images. Because of space constraints, only a few are presented here (Figs. 4–7). However, the data from all of the images were used for calculation of degree of unmixedness, which in turn was used for determining the mixing lengths.

It can be seen from the images that as the flow progresses streamwise the injected streams get mixed with the crossflow. This results

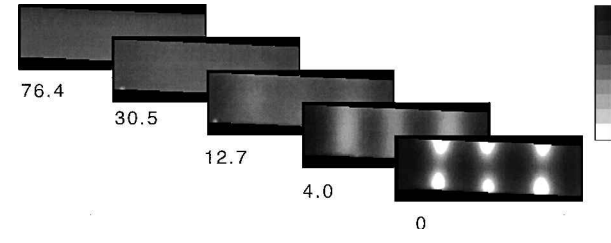

Fig. 4 PLIF images of a few cross sections: configuration 1, hole diameter 0.7 mm, momentum ratio 16.4, and mass ratio 0.35. Mixing length calculated is 10.3 mm. (The image locations are given in millimeters.)

in the intensities becoming uniform throughout the image. Therefore, the nonuniformity of intensities in the image (represented by the variance) decreases at downstream locations as compared to upstream locations.

It can be noted from the images that for some high-injection pressures the jets impinge head on onto each other. This occurrence was also noted by Elior et al.[28] and Bain et al.[3] This could be attributed to the higher momentum of the jets when compared to the crossflow. When the jets impinge on each other at the injection location, they spread very fast in the transverse direction and almost completely fill the test section. Often, near-uniform mixing is achieved at the injection location and takes only a small distance downstream to mix uniformly.

It is interesting to observe the images of the mole fraction distributions for a case with very slight change in the injection pressure to effect a weak impingement of jets. The injection pressure for the former case was 7 torr and for the latter was 7.8 torr. The corresponding momentum ratios for the two cases were 23.2 and 25.9. It can be seen from Fig. 8 that in the latter case the jets impinge head on onto each other.

The plots of degree of unmixedness for these cases are given in Fig. 9. It can be seen that the mixing is faster for the case where the jets impinge. The degree of unmixedness is lesser to start with. The mixing length (determination of mixing length will be explained in the next section) for the nonimpinging case was 12.6 mm and for the impinging case was 4.9 mm. Thus impingement of the jets improves their mixing.

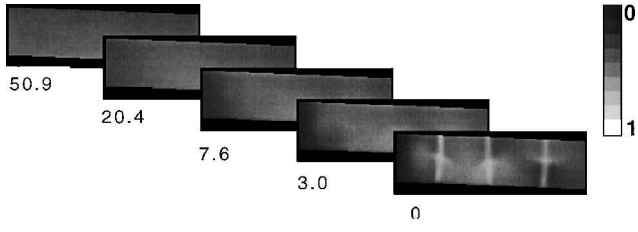

Fig. 5 PLIF images of a few cross sections: configuration 1, hole diameter 0.7 mm, momentum ratio 29.1, and mass ratio 0.62. Mixing length calculated is 8.0 mm. (The image locations are given in millimeters.)

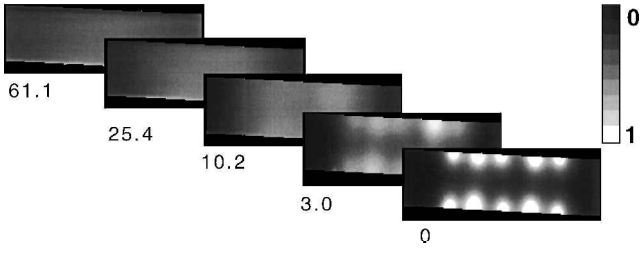

Fig. 6 PLIF images of a few cross sections: configuration 2, hole diameter 0.7 mm, momentum ratio 27.3, and mass ratio 0.58. Mixing length calculated is 15.3 mm. (The image locations are given in millimeters.)

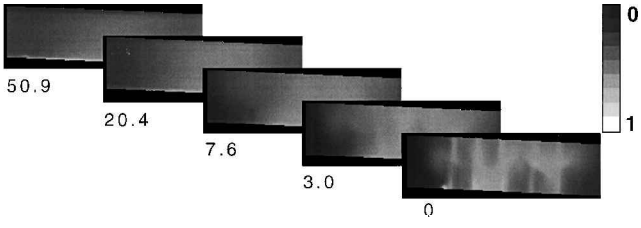

Fig. 7 PLIF images of a few cross sections: configuration 2, hole diameter 0.7 mm, momentum ratio 65.8, and mass ratio 1.16. Mixing length calculated is 8.4 mm. (The image locations are given in millimeters.)

Determination of Mixing Lengths

The objective of this study is to quantify the mixing of transversely injected jets with a crossflow in low density conditions. Therefore a mixing length, that is, the distance downstream of injection plane after which the flow is considered fully mixed, had to be determined from the images.

For obtaining this, the degree of unmixedness was obtained at various streamwise locations. The flow was considered "mixed" at a location downstream of which the degree of unmixedness is less than 0.05. Figure 10 illustrates the determination of the mixed condition.

Data Analysis

It can be observed from these images that for the same injection flow rate the mixing distance increases with the increase in the crossflow velocity. This is caused by the axial convection being more predominant for higher crossflow velocities. It is also seen that for a constant crossflow velocity the mixing distance decreases with increase in the injection pressure as a result of increase in transverse momentum.

The mixing lengths obtained were correlated using the ratio between the total momentum flow rate of the injected jets and that of the crossflow. The mixing lengths were linearly dependent on this ratio until a value beyond which the jets mix with the crossflow at the injection location itself (Fig. 11). It can be seen from this

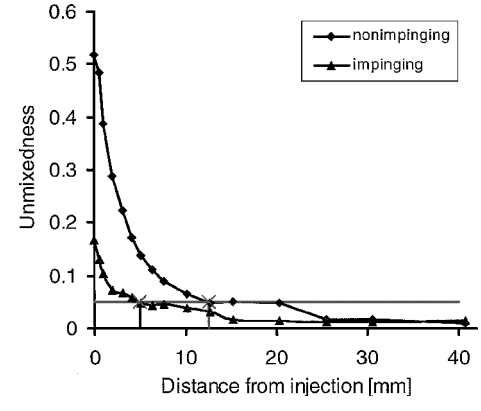

Fig. 9 Streamwise variation of unmixedness for impinging and nonimpinging cases as shown by images in Fig. 8. Degree of unmixedness is reduced drastically by making the jets impinge on each other. Also, the mixing length is decreased considerably.

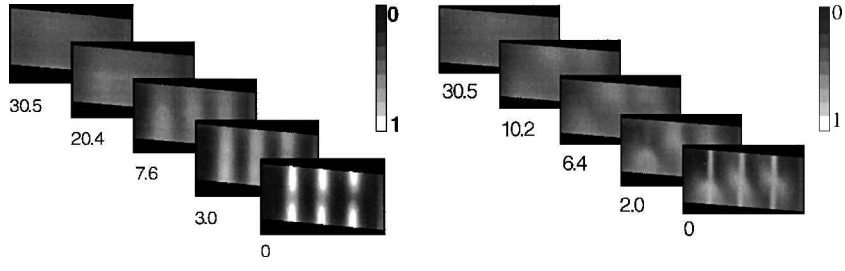

Fig. 8 Comparison of nonimpinging (left) and impinging (right) jets. Left-hand image gives mapping of mole fractions for condition with 7-torr injection pressure, and the right-hand image is for 7.8 torr with all other parameters maintained constant. Momentum ratios were 23.2 and 25.9, respectively. Mixing lengths were 12.6 and 4.9 mm, respectively. (The image locations are given in millimeters.)

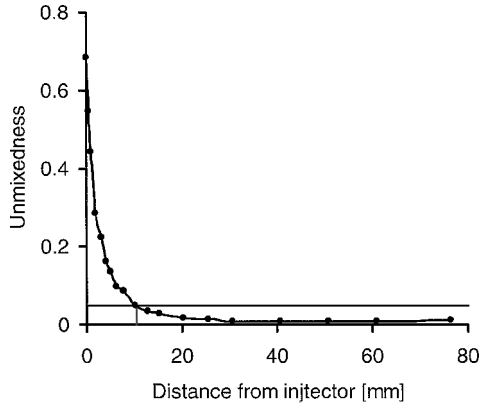

Fig. 10 Determination of mixing length from variation of unmixedness. The point where the unmixedness value crosses 0.05 is defined as the mixing length in this study. This case shown had a mixing length of 10.3 mm.

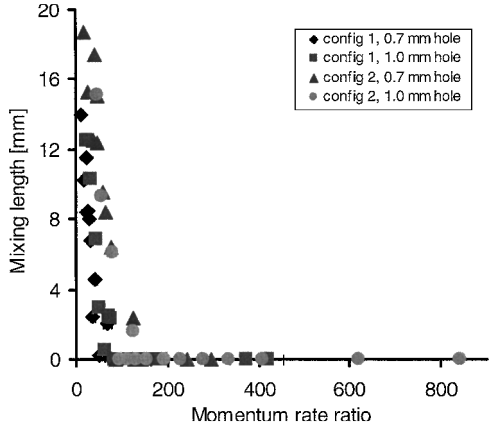

Fig. 11 Mixing lengths as a function of momentum rate ratio for all of the cases investigated in this study.

figure that the mixing length depends on the momentum rate ratio. Also, there are many points with zero or near-zero mixing lengths (which implies mixing at the injection plane).

This case of zero or near-zero mixing length is quite different from the classical results of jet mixing in a crossflow at atmospheric or higher pressures. It can be explained by the fact that the jets are having very high momentum compared to the crossflow and also the experiment takes place in a low-pressure environment. The jets are underexpanded, and therefore they can spread faster.

Also, their high momentum causes the jets to impinge and distribute mass upstream of the injection point, which then is redistributed by the streamwise vorticity. And the stronger diffusion effects at low pressures help in this expedited mixing event. Because this is creeping flow (as a result of very low pressures; $Re_{\text{crossflow}} = 4$–12, height of the test section being the characteristic dimension), the vorticity produced will be diffused very quickly, and thus only very near the injection plane do we have the vorticity based mixing. Classical kidney-shaped cross sections observed at higher pressures do not appear in this flow for the same reason. Also, the high mass diffusion in low-pressure conditions will smooth out any sharp gradients in the flow, which gives the jets a cloudy edge as compared to atmospheric pressure jets in cross flow. This smudged kidney-shaped structures can be seen in Figs. 4 and 6.

To better understand the functional dependence of the mixing length on the momentum rate ratio, the points of zero mixing length were removed from the graph, and the rest of the points are plotted in Fig. 12. This plot shows that the linearity is specific to the injector hole configuration, and thus the two configurations considered give two different correlations. The two type of injector configurations considered are illustrated in Fig. 2.

The correlations for the mixing lengths as a function of momentum ratio are given for the two cases investigated here.

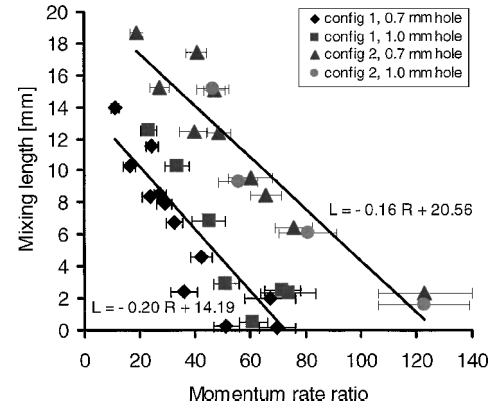

Fig. 12 Nonzero mixing lengths as a function of momentum ratio. The two injector configurations give two different correlations. Diameter of the holes does not change the mixing lengths by a lot.

Configuration 1:

$$L = -0.20R + 14.19$$

Configuration 2:

$$L = -0.16R + 20.56$$

where R is the momentum rate ratio and L is the mixing length. The correlation coefficients are 0.76 and 0.88, respectively. This correlation will be duct specific and thus is valid only for a 10×50 mm duct with these injector configurations or a scaled version of this. At momentum ratios of 71 and 128.5, respectively, the graphs touch zero; that is, the mixing length is zero, or in other words mixing occurs at the injection plane.

This quantitative relation is most helpful in the design of the nitrogen-diluted subsonic COIL (with a diluent ratio of around 4:1) by giving the approximate location of the laser cavity. This distance given by the relation is approximate because this experimental study did not involve any reacting flow or lasing unlike the actual COIL. There will be a small variation in the required optimum location of the cavity as the mixing length can be altered slightly by heat release in the reaction and change in molecular composition as a result of consumption of iodine. When the diluent ratio in the main flow is changed, the results will not be altered much because the major fluid mechanic parameters will not be affected by replacing nitrogen with oxygen.

Also, impingement of the jets might have an effect on the consumption of iodine molecules. Impingement of the jets will be associated with a pressure drop because of blockage of the duct, but it is already accounted for in this correlation.

The various issues in this mixing problem are as follows. The entire flow is at low pressure so that diffusive transport is the main mixing mechanism. However, very near the injector array the inertial mechanism will be stronger than the diffusive mechanism as a result of the high velocities of injection. This vorticity produced near the injector array is quickly dissipated by this creeping flow. Thus the hole diameter will affect the mixing very close to the injector, but far away the mixing is purely diffusive. Thus, overall, the mixing length depends mainly on the amount of mass injected and how distributed the injector configuration is spatially.

Momentum ratio and mass ratio are the important parameters governing the mixing length. In this situation, because the injection is choked, the mass ratio and the momentum ratio are directly related with a small deviation from linear relation caused by the pressure variations in the test section (crossflow density variations). This means that the mixing lengths can be correlated with mass ratio as well as momentum ratio. Because for a few cases the mixing lengths are very small and thus momentum mixing is important, the momentum rate ratio correlation is more useful here.

The injector hole diameter plays only a small role in the mixing process and thus is not an important parameter in this low-pressure mixing problem. This is clearly seen from Fig. 12, where the mixing

Table 1 Select set of cases from the full data set to show the dependence on hole diameter and the configuration (all ratios are jet-to-crossflow ratios)

Case	Configuration	Hole diameter, mm	Density ratio	Mass ratio	Momentum rate ratio	Mixing length, mm
1	2	0.7	3.53	0.97	47.04	15.0
2	2	1	1.82	0.99	46.64	15.1
3	2	0.7	3.90	1.03	48.51	12.4
4	2	0.7	2.19	0.58	27.29	15.3
5	1	0.7	3.63	0.58	27.42	8.5

length data for the two hole diameter cases coincide to give a single correlation for each injector configuration (the spatial distributedness of the injector array).

Cases 1 and 2 in Table 1 are both 1-mm hole arrays in configuration 2 and result in approximately same mass flow ratio and momentum rate ratio and thus have the same mixing length even though the hole diameters are different. Also from cases 2 and 3 we see that for a given mass flow ratio the mixing length variation with momentum ratio is as given by the correlation already presented in this paper. This shows that the dependence on the hole diameter is minimal and the main parameter is the momentum rate ratio. This would imply that a designer can replace a smaller diameter hole with a slightly bigger hole for easy manufacturability and adjust the injection pressure to get the same mass ratio and momentum ratios to get the same desired mixing.

To see the effect of the injector hole configuration, consider cases 4 and 5 in Table 1. Both the cases have the same mass ratio and the momentum ratio but are of different configurations. We see that configuration 2 has a higher mixing length compared to configuration 1. This shows that the mixing length depends on the spatial distribution of the holes in the injector array and is lesser for spatially uniform configurations.

Though this study was performed in the context of subsonic COIL, the main focus was on the fluid mechanics of mixing in the low-pressure conditions in a typical subsonic COIL. Because there is very little literature about low-pressure mixing studies, these data would help in preliminary design of a subsonic COIL. Also for the same reason this work can be used to benchmark CFD results for low-pressure mixing studies.

Conclusions

The mixing of transversely injected jets of a carrier gas carrying iodine vapor with a crossflow under low-density condition was investigated using planar-laser-induced iodine fluorescence. The dependence of the mixing length on crossflow and injector parameters was investigated.

A parameter called degree of unmixedness, defined based on the variance of intensities of fluorescence at each downstream cross section, was used to quantify mixing. A mixing length was defined as the location downstream of which the degree of unmixedness was less than 0.05. It was found that when the jets impinge head on with the opposed jet the unmixedness values are low to start with and thus mixing lengths are small.

The mixing lengths obtained were correlated using the ratio between the momentum flow rates of the injected jets and the crossflow. The mixing lengths were linearly dependent on this ratio until a value where the jets mixed at the injection location. This linearity is specific to the injector configuration, and thus the two configurations considered give two different correlations.

The correlations for the mixing lengths as a function of momentum ratio were obtained for the two cases investigated in this work. This correlation is more or less independent of the hole diameter. Thus a designer can inject the same mass flow through the injectors with lower pressures and bigger holes instead of higher pressures and smaller holes.

The effect of the number of holes on the mixing length is governed by the correlations obtained in this work. The closely spaced, spatially concentrated injector hole configuration has a longer mixing length than the spatially distributed hole configuration because diffusion is the governing mixing mechanism.

The data obtained in this study can be used for designing an efficient nitrogen diluted subsonic COIL. However, the effects of reactions were not considered in this study. This study could also serve as a benchmark for the CFD programs used for prediction of mixing of jet in crossflow in low-pressure environments. The concentration maps presented here can also be used for checking the predictions from CFD codes.

Acknowledgments

This work was funded by the Board of Research for Nuclear Sciences. The authors would like to thank D. Bhawalkar and U. Nundy and his group at the Center for Advanced Technologies, Indore, who had shown a great deal of interest in the progress of this work. The help from T. P. S. Nathan and his group at the Center for Advanced Technologies in maintaining the Nd-YAG laser is greatly appreciated.

References

[1]Margason, R. J., "Fifty Years of Jet in Cross Flow Research," *Computational and Experimental Assessment of Jets in Cross Flow*, CP 534, AGARD, April 1993.

[2]Holdeman, J. D., "Mixing of Multiple Jets with a Subsonic Cross Flow," *Progress in Energy and Combustion Science*, Vol. 19, 1993, pp. 31–70; also AIAA Paper 91-2458, June 1991.

[3]Bain, D. B., Smith, C. E., Liscinsky, D. S., and Holdeman, J. D., "Flow Coupling Effects in Jet-in-Crossflow Flowfields," *Journal of Propulsion and Power*, Vol. 15, No. 1, 1999, pp. 10–16.

[4]Bain, D. B., Smith, C. E., and Holdeman, J. D., "Mixing Analysis of Axially Opposed Rows of Jets Injected into Confined Crossflow," *Journal of Propulsion and Power*, Vol. 11, No. 5, 1995, pp. 885–893; also AIAA Paper 93-2044, June 1993.

[5]Blomeyer, M. M., Krautkremer, B. H., and Hennecke, D. K., "Optimum Mixing for a Two-Sided Injection from Opposed Rows of Staggered Jets in a Confined Crossflow," International Gas Turbine and Aeroengine Congress and Exhibition, American Society of Mechanical Engineers, Paper 96-GT-483, June 1996.

[6]Chiu, S., Roth, K. R., Margason, R. J., and Tso, J., "A Numerical Investigation of a Subsonic Jet in Crossflow," AIAA Paper 93-0870, Jan. 1993.

[7]Doerr, T., Blomeyer, M., and Henneke, D. K., "Optimization of Multiple Jets Mixing with a Confined Crossflow," International Gas Turbine and Aeroengine Congress and Exhibition, American Society of Mechanical Engineers, Paper 95-GT-313, June 1995.

[8]Liscinsky, D. S., True, B., and Holdeman, J. D., "Experimental Investigation of Crossflow Jet Mixing in a Rectangular Duct," AIAA Paper 93-3090, July 1993.

[9]Liscinsky, D. S., True, B., and Holdeman, J. D., "Mixing Characteristics of Directly Opposed Rows of Jets Injected Normal to a Cross Flow in a Rectangular Duct," AIAA Paper 94-0217, Jan. 1994.

[10]Holdeman, J. D., Liscinsky, D. S., and Bain, D. B., "Mixing of Multiple Jets with a Confined Subsonic Cross flow: Part II—Opposed Rows of Orifices in Rectangular Ducts," *Journal of Engineering for Gas Turbines and Power*, Vol. 121, No. 3, 1999, pp. 551–562.

[11]Avizonis, P. V., and Truesdell, K. A., "Historical Perspectives of the Chemical Oxygen Iodine Laser (COIL)," AIAA Paper 94-2416, June 1994.

[12]Avizonis, P. V., Hasen, G., and Truesdell, K. A., "The Chemically Pumped Oxygen Iodine Laser," *High Power Gas Lasers*, Vol. 1225, edited by P. V. Avizonis, C. Freed, J. J. Kim, and F. K. Tittel, Society of Photo-Optical Instrumentation Engineers, Bellingham, WA, 1990, p. 448.

[13]Stepanov, A. A., Scheglov, V. A., and Yuryshev, N. N., "Continuous Wave Transfer Chemical Lasers (Review)," *Soviet Journal of Quantum Electronics*, Vol. 15, No. 6, 1985, p. 746.

[14]Barmashenko, B. D., Elior, A., Leblush, E., and Rosenwaks, S., "Modeling of Mixing in Chemical Oxygen Iodine Lasers: Analytical and Numerical Solutions and Comparison with Experiments," *Journal of Applied Physics*, Vol. 75, No. 12, 1994, p. 7653.

[15]Barmashenko, B. D., and Rosenwaks, S., "Power Dependence of Chemical Oxygen–Iodine Lasers on Iodine Dissociation," *AIAA Journal*, Vol. 34, No. 12, 1996, pp. 2569–2574.

[16]Madden, T. J., Caroll, D. L., and Solomon, W. C., "Detailed Mixing in COIL Devices," AIAA Paper 94-2432, June 1994.

[17]Carroll, D. L., "Modeling High-Pressure Chemical Oxygen–Iodine Lasers," *AIAA Journal*, Vol. 33, No. 8, 1995, pp. 1454–1462.

[18]Madden, T. J., Caroll, D. L., and Solomon, W. C., "An Investigation of High Pressure COIL Performance Improvement Methods Using CFD," AIAA Paper 96-2354, June 1996.

[19]Hanson, R. K., "Combustion Diagnostics : Planar Imaging Techniques," *Proceedings of the 21st Symposium (International) on Combustion*, Combustion Inst., Pittsburgh, PA, 1986, p. 1677.

[20]Hiller, R., and Hanson, R. K., "Properties of Iodine Molecule Relevant to Laser-Induced Fluorescence Experiments in Gas Flows," *Experiments in Fluids*, Vol. 10, No. 1, 1990, p. 1.

[21]McDaniel, J. C., Hiller, B., and Hanson, R. K., "Simultaneous Multiple-Point Velocity Measurements Using Laser-Induced Iodine Fluorescence," *Optics Letters*, Vol. 8, No. 1, 1983, p. 51.

[22]Hartfield, R. J., Abbitt, J. D., and McDaniel, J. C., "Injectant Mole-Fraction Imaging in Compressible Mixing Flows Using Planar Laser-Induced Iodine Fluorescence," *Optics Letters*, Vol. 14, No. 16, 1989, p. 850.

[23]Bohn, W. L., "COIL Activities in Germany," *Proceedings of 4th International Workshop on Iodine Lasers and Applications*, edited by K. Rohlena, J. Kodymova, and B. Krakilova, Society of Photo-Optical Instrumentation Engineers, Bellingham, WA, 1995.

[24]Schall, W. O., "Experiments and Modeling of Iodine Oxygen Mixing in Supersonic COILs," *Proceedings of the 3rd International Workshop on Iodine Lasers and Applications*, Vol. 1980, edited by M. Chvojka, J. Kodymova, and B. Krakilova, Society of Photo-Optical Instrumentation Engineers, Bellingham, WA, 1992, p. 170.

[25]Schlichting, H., *Boundary Layer Theory*, translated by J. Kestin, McGraw–Hill, New York, 1960, Chap. 9.

[26]Wang, K. C., Smith, O. I., and Karagozian, A. R., "In-Flight Imaging of Transverse Gas Jets Injected into Compressible Crossflows," *AIAA Journal*, Vol. 33, No. 12, 1995, pp. 2259–2263.

[27]Philips, D., *Image Processing in C*, BPB Publications, New Delhi, India, 1995, Chap. 7.

[28]Elior, A., Barmashenko, B. D., Lebiush, E., and Rosenwaks, S., "Experiment and Modeling of a Small-Scale, Supersonic Chemical Oxygen-Iodine Laser," *Applied Physics B*, Vol. 61, No. 1, 1995, pp. 37–47.

R. P. Lucht
Associate Editor